

Microwave synthesis and studies room temperature optical properties of LaF₃: Ce³⁺, Pr³⁺, Nd³⁺ nanocrystals

Sidheshwar G Gaurkhede

Department of Physics, Bhavan's College of Science, Andheri (W) Mumbai – 400058, India

s.gaurkhede@gmail.com

PACS 61.05.cp, 77.22.d

DOI 10.17586/2220-8054-2020-11-1-117-122

Lanthanum fluoride (LaF₃:Ce³⁺, Pr³⁺, Nd³⁺) was synthesized by water soluble LaCl₃ + CeCl₃ + PrCl₃ + NdCl₃ and NH₄F as starting materials in de-ionized water as solvent using microwave assisted technique. The structure of LaF₃:Ce³⁺, Pr³⁺, Nd³⁺ nanocrystals analyzed by XRD and TEM analysis is found to be in hexagonal structure and average crystalline particle size is 20 nm (JCPDS standard card (32-0483) of pure hexagonal LaF₃ crystals). The absorption edge in UV spectra is found at 250 nm corresponding to energy of 4.9 eV. It further shows a wide transparent window lying between 200 nm–800 nm. For LaF₃: Ce³⁺, Pr³⁺, Nd³⁺ nanocrystals emission of blue color (458 nm) has been observed with at an excitation wavelength of 254 nm. The measured relative second harmonic generation (SHG) efficiency of LaF₃: Ce³⁺, Pr³⁺, Nd³⁺ in de-ionized water with respect to KDP crystal is 0.186.

Keywords: Microwave radiation, Hexagonal shape, X-ray diffraction, Luminescent, SHG.

Received: 23 January 2020

1. Introduction

LaF₃ is an ideal host material for various phosphors to its low phonon energy and the consequent minimal multi phonon relaxation of its excited states [1, 2]. Lanthanum fluoride is an excellent F⁻ ionic conductor among other rare earth fluorides [3]. Lanthanum fluoride based chemical sensors widely used in potential application in sensing the fluorine, oxygen, and carbon monoxide due to its high chemical stability and ionic conductivity [4]. Ion conducting nature of the rare earth fluorides (solid electrolyte) is exploited as sensor materials to construct various electrochemical sensors like gas sensor, biosensor, and ion selective electrode [5]. Miura et al. reported the use of lanthanum fluoride film in biosensor and room-temperature oxygen sensor based on its high F⁻ ion-conducting property. The working principle of LaF₃ based biosensor and oxygen sensors is explained as the movement of F⁻ ion conduction [6, 7]. Fedorov P.P. [8] et al. review the major aspects of inorganic chemistry of nanofluorides, methods of synthesis including nanochemical effects, preparation of 1D, 2D, and 3D nanostructures, surface modification of the nanoparticles, fluoride nanocomposites and applications of nanofluorides. The orthorhombic β -YF₃ structure and ionic conductivity of rare earth fluorides and of tysonite-structured were investigated by Trnovcova et al. [9, 10].

Hai Guo et al. [11] have reported water-soluble LaF₃: Ce³⁺, Tb³⁺ nanodiskettes having particle size of 25 nm synthesized by ionic liquid-based hydrothermal process. The luminescent properties of LaF₃: Ce³⁺, Tb³⁺ nanodiskettes show intense green emission (541 nm) at 254 nm excited wavelength both in solid state and dispersed in solution. A simple and straightforward method was developed by Yong Zhang et al. [12, 13] to produce water-dispersible LaF₃: Ce³⁺, Tb³⁺ nanocrystals and to grow these nanocrystals on silica microspheres which show a raspberry-like structure with LaF₃ nanocrystals. The nanocrystals were 25 nm in size and exhibited strong green fluorescence for excited wavelength of 254 nm. There is a report by Cong-Cong Mi et al. [14] on Polyethyleneimine (PEI) functionalized multicolor luminescent LaF₃: Ce³⁺, Tb³⁺ nanoparticles which were synthesized via a novel microwave-assisted method and nanoparticles possessed a pure hexagonal structure with an average size of was 12 nm and green fluorescence was observed when sample was excited with 252 nm wavelength. The lanthanide series of trivalent ions is Ce³⁺, Pr³⁺, Nd³⁺ having ultra violet (UV) and visible luminescence spectra consisting of many narrow lines whose half-widths reach only several nm⁻¹. It was found that the in Nd³⁺ UV and visible luminescence depend on the excitation wavelength [15].

The synthesized LaF₃:Ce³⁺, Pr³⁺, Nd³⁺ nanoparticles exhibit hexagonal shape and exhibit blue luminescence. In the present case LaF₃:Ce³⁺, Pr³⁺, Nd³⁺ nanoparticles have been synthesized using a conventional microwave radiation technique for first time.

2. Experimental

2.1. Synthesis of nanocrystals

Synthesis of $\text{LaF}_3:\text{Ce}^{3+}$, Pr^{3+} , Nd^{3+} nanocrystals follows an aqueous route and uses a microwave heating at low power range. The method is simple and cost effective. Water soluble $\text{LaCl}_3 + \text{CeCl}_3 + \text{PrCl}_3 + \text{NdCl}_3$ and NH_4F are mixed to obtain a solution in 1:3 molar proportions [16]. A 10 ml homogenous mixture (in the ionized water) in a 100 ml beaker using 0.064 mol of each $\text{LaCl}_3 + \text{CeCl}_3 + \text{PrCl}_3 + \text{NdCl}_3$ allowed a 10 ml solution of 0.768 mol NH_4F to drip into this solution uniformly through a funnel attached with a stopper to facilitate control of dripping, and placed the whole set up inside a conventional microwave set at low power range (in on-off mode set at 30 sec) for around 30 min. The low power range setting largely helped us avoid spill off of the solution. A white crystalline precipitate identified as doped LaF_3 nanocrystals appears almost instantly having settled down to the bottom of the beaker. White precipitate is then washed several times with de-ionized water and then drying it in microwave oven for about 15 min. The dried sample was then stored in sealed ampoules for further characterization and analysis.

3. Characterization

Powder X-ray diffraction (XRD) measurements have been performed using a PANALYTICAL X'PERT PROMPD diffractometer model using $\text{CuK}\alpha$ radiation $\lambda = 1.5405 \text{ \AA}$ with a scanning rate of 20 per min in the 2° range from 0° to 80° . Transmission electron microscope (TEM) analysis has been carried out for different magnification by PHILIPS (CM 200) 0.24 nm resolution, operating at 200 kV. The UV-visible spectrum of the samples was recorded in the spectral range of 200 nm–800 nm using a double beam (Perkin Elmer Corp.) spectrophotometer. The fluorescence spectrum was measured on LS 45 luminescence spectrometer (Perkin Elmer Corp.) using a high energy pulsed Xenon source for excitation and FL Win Lab software. NLO studies for the measurements of SHG efficiency are obtained through the crystalline powder sample by using Kurtz and Perry technique.

4. Result and discussion

The XRD pattern obtained from the $\text{LaF}_3:\text{Ce}^{3+}$, Pr^{3+} , Nd^{3+} nanocrystals shown in Fig. 1. The results of the XRD are in good agreement with the hexagonal LaF_3 structure as described in the reports LaF_3 (JCPDS card No. 32-0483) [17]. The average crystallite size estimated from the Scherrer equation, $D = 0.90\lambda/\beta \cos \theta$, where D is the average crystallite size, λ is the x-ray wavelength (0.15405 nm), θ and β being the diffraction angle and full width at half maximum of an observed peak, respectively. The strongest peak (111) at $2\theta=27.84^\circ$ for $\text{LaF}_3:\text{Ce}^{3+}$, Pr^{3+} , Nd^{3+} samples have been used to calculate the average crystallite size (D) of the nanoparticles [18]. The average crystallite sizes of $\text{LaF}_3:\text{Ce}^{3+}$, Pr^{3+} , Nd^{3+} nanoparticles are in the range of 15 nm–20 nm, which is in agreement with the TEM and SEM results. The XRD pattern of the LaF_3 nanoparticles is nearly similar to that of $\text{LaF}_3:\text{Ce}^{3+}$, Tb^{3+} [19]. No XRD signals are observed for impurity phases.

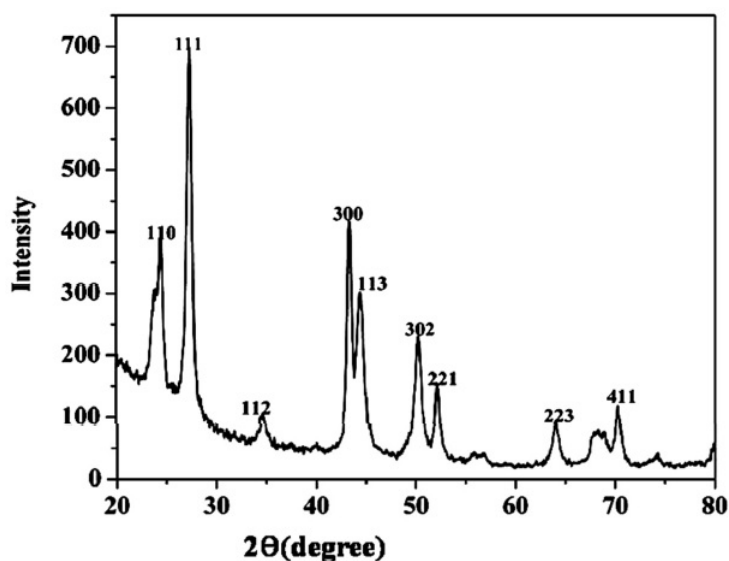


FIG. 1. X-ray diffraction pattern of $\text{LaF}_3:\text{Ce}^{3+}$, Pr^{3+} , Nd^{3+} nanocrystals

Figure 2 shows the transmission electron microscopy (TEM) image of $\text{LaF}_3: \text{Ce}^{3+}, \text{Pr}^{3+}, \text{Nd}^{3+}$ nanocrystals. It is seen that most of the nanocrystals are in the form of hexagon, sphere and nanorods. Most of the nanorods of $\text{LaF}_3: \text{Ce}^{3+}, \text{Pr}^{3+}, \text{Nd}^{3+}$ are found to be well separated with some instances of agglomeration with average particle size of 20 nm are found. Fig. 3 shows the selected area electron diffraction (SAED) pattern. Three strong diffraction rings corresponding to the (002), (111) and (300) reflections, have been observed which is in close agreement with the hexagonal LaF_3 structure [20]. This shows that the original structure of LaF_3 may be retained even after modification.

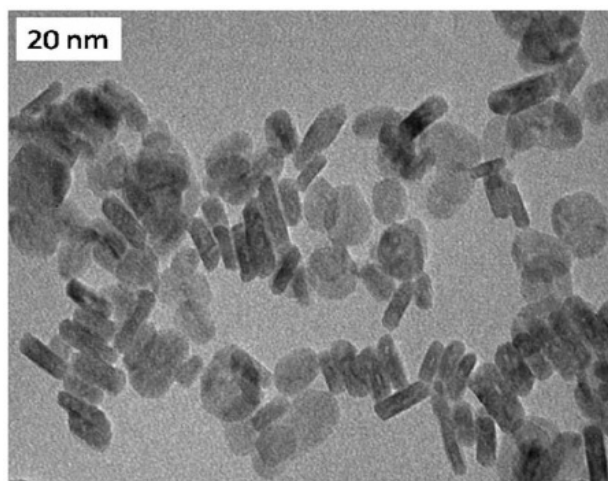


FIG. 2. TEM image of $\text{LaF}_3: \text{Ce}^{3+}, \text{Pr}^{3+}, \text{Nd}^{3+}$ nanocrystals

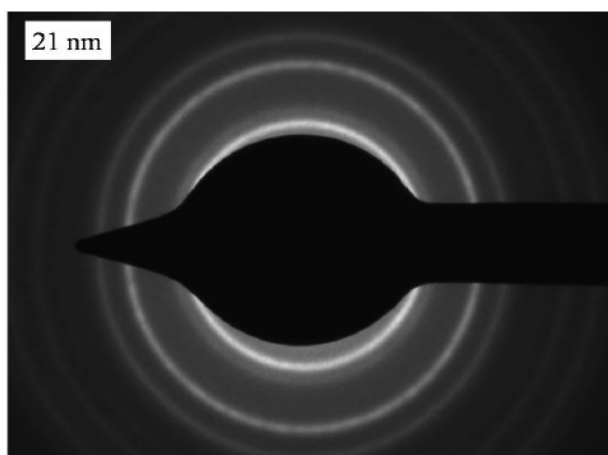


FIG. 3. Selected area electron diffraction (SAED) pattern image of $\text{LaF}_3: \text{Ce}^{3+}, \text{Pr}^{3+}, \text{Nd}^{3+}$ nanocrystals

Figure 4 shows the optical absorption spectrum of the nanocrystallites with an absorption edge at 250 nm in the UV region, with corresponding energy band gap lying at 4.9 eV. Absorption against wavelength values was used to determine the band gap energy. The band gap energy was calculated by determining the ' $h\nu$ ' value. A wide transparent window is present between 200 – 800 nm suggesting its use in optoelectronics devices.

The emission spectra of synthesized $\text{LaF}_3: \text{Ce}^{3+}, \text{Pr}^{3+}, \text{Nd}^{3+}$ ion is shown in Fig. 5. The emission spectra was obtained by monitoring (254 nm) 4f to 5d transition of Ce^{3+} ions. The broadband emission is located at 458 nm due to the electronic transitions from 5d to 4f state of Ce^{3+} ions [21]. The sharp emission peaks originates from the 4f5d - 4f² transitions of Pr^{3+} ions [$^3\text{H}_4 \rightarrow ^3\text{P}_2$ (458 nm), $^3\text{H}_4 \rightarrow ^3\text{P}_0$ (497 nm), $^3\text{H}_4 \rightarrow ^1\text{D}_2$ (608 nm)]. The quenching of Ce^{3+} emissions and the enhancement of Pr^{3+} emissions is strong evidence of efficient energy transfer from Ce^{3+} to Pr^{3+} and Nd^{3+} . The emission spectrum is mainly located in the region corresponding to blue colour. Here, the doping Ce^{3+} ions act as sensitizers and the doping ions $\text{Pr}^{3+}, \text{Nd}^{3+}$ can be considered as luminescent centers. It is well known fact that the luminescent spectra of trivalent lanthanide ions in crystals come mainly from two types of electronic transitions: 4f-4f transition and 5d-4f transition. The excited electronic configuration of Ce^{3+} is $^5\text{D}_1$. The

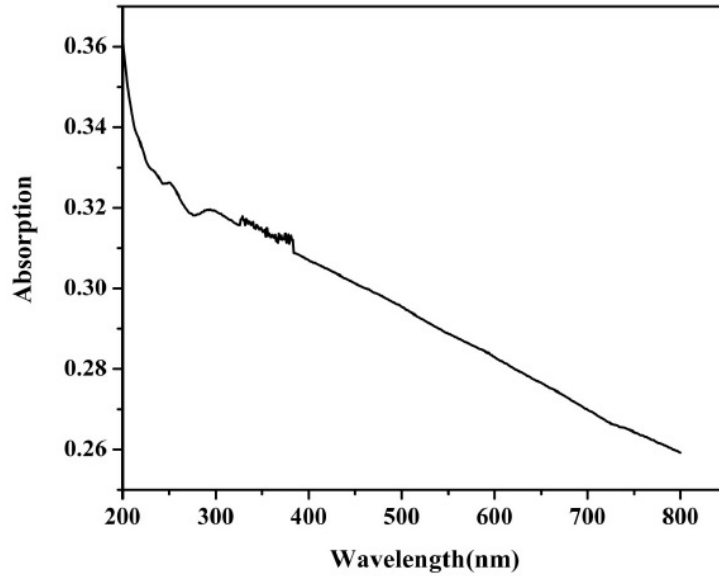


FIG. 4. UV-VIS absorption spectra of LaF_3 doped Ce^{3+} , Pr^{3+} Nd^{3+} nanocrystals in ionized water

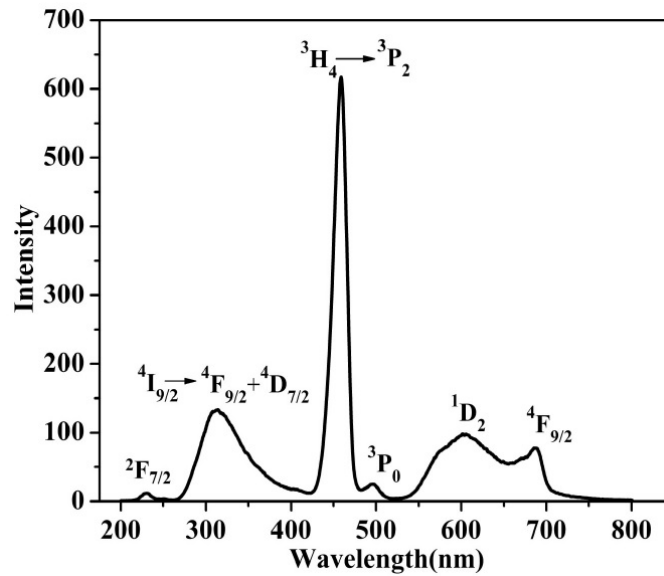
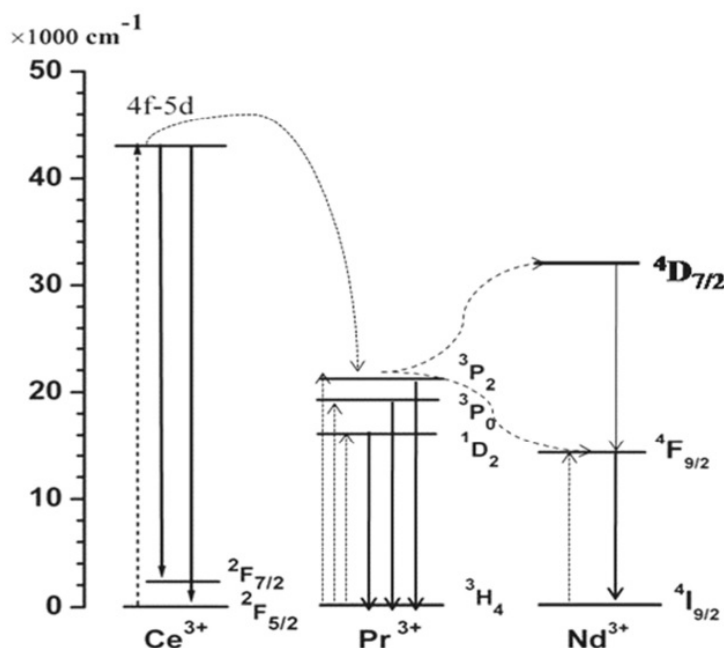


FIG. 5. Excitation ($\lambda_{em}=458$ nm) and Emission ($\lambda_{ex}=254$ nm) spectra of LaF_3 nanocrystals doped Ce^{3+} , Pr^{3+} , Nd^{3+} ions in deionized water

5d electron has a strong interaction with the neighboring anion ligands in the compounds and results in broadband emissions. The 4f orbital is shielded from the surroundings by the filled $5s^2$ and $5p^6$ orbital. Therefore, the influence of the host lattice on the optical transitions within the $4f^n$ configuration is small [15, 22].

Figure 6 shows the energy level scheme of LaF_3 ; Ce^{3+} , Pr^{3+} Nd^{3+} , with optical transitions and energy transfer processes. The Ce^{3+} ion excited at 254 nm absorbs one photon and is pumped to the 5d level. Then, it relaxes to the ground state by radiative process with emission of photons; and transfers its energy to a nearby Pr^{3+} ion in the ground state, promoting this Pr^{3+} ion to excited state. Then, the excited Pr^{3+} ion relaxes to the $^3\text{P}_2$, $^3\text{P}_0$, and $^1\text{D}_2$ levels by non-radiative process. The Pr^{3+} ion excited by 254 nm is pumped to the $^3\text{P}_2$, $^3\text{P}_0$, and $^1\text{D}_2$ states. As mentioned above, $^3\text{H}_4 \rightarrow ^3\text{P}_2$ (458 nm), $^3\text{H}_4 \rightarrow ^3\text{P}_0$ (497 nm), $^3\text{H}_4 \rightarrow ^1\text{D}_2$ (608 nm) transitions have been observed only for low Pr^{3+} doped samples. Blue fluorescence from the higher energy $^3\text{P}_2$ level has been observed for high Pr^{3+} doped samples [23].


 FIG. 6. Energy level scheme for $\text{LaF}_3: \text{Ce}^{3+}, \text{Pr}^{3+}, \text{Nd}^{3+}$ nanocrystals

The nonlinear optical property of $\text{LaF}_3: \text{Ce}^{3+}, \text{Pr}^{3+}, \text{Nd}^{3+}$ in de-ionized water was tested by passing the output of Nd: YAG Quanta ray laser emitting 1064 nm, generating about 6mJ / pulse through the samples. SHG is a key technology as frequency doublers of laser light. The SHG efficiency of $\text{LaF}_3: \text{Ce}^{3+}, \text{Pr}^{3+}, \text{Nd}^{3+}$ nanocrystals were determined in de-ionized water by modified Kurtz and Perry technique [24]. Crystalline powder of Potassium dihydrogen phosphate (KDP) taken as the reference material. The measured relative SHG efficiency of $\text{LaF}_3: \text{Ce}^{3+}, \text{Pr}^{3+}, \text{Nd}^{3+}$ in de-ionized water with respect to KDP crystal is 0.186.

5. Conclusions

LaF_3 nanocrystals successfully have been synthesized using $\text{LaCl}_3 + \text{CeCl}_3 + \text{PrCl}_3 + \text{NdCl}_3$ and NH_4F in deionized water. Elongated and assorted size hexagonal geometry of LaF_3 nanocrystals has been observed. XRD and TEM studies indicate that the average particle size is 20 nm. The conductivity at room temperature for LaF_3 sample prepared in deionized water is found to be in close agreement with reported values. The absorption edge in UV spectra is found at 250 nm corresponding to energy of 4.9 eV. It further shows a wide transparent window lying between 200 nm–800 nm. For $\text{LaF}_3: \text{Ce}^{3+}, \text{Pr}^{3+}, \text{Nd}^{3+}$ nanocrystals emission of blue color (458 nm) has been observed with an excitation wavelength of 254 nm. The SHG property was tested by using Nd: YAG laser. The second harmonic efficiency of $\text{LaF}_3: \text{Ce}^{3+}, \text{Pr}^{3+}, \text{Nd}^{3+}$ nanocrystals is found to be 0.186 in deionized water using KDP as standard material.

References

- [1] Zheng H.R. Up-converted emission in Pr^{3+} doped fluoride nanocrystals-based oxyfluoride glass ceramics. *Journal of Luminescence*, 2004, **108**(1), P. 395–399.
- [2] Nogami M. Enhanced fluorescence of Eu^{3+} induced by energy transfer from nanosized SnO_2 crystals in glass. *Journal of Luminescence*, 2002, **97**(3), P. 147–152.
- [3] Schoonman J., Oversluizen G., Wapennar K.E.D. Solid electrolyte properties of LaF_3 . *Solid State Ionics*, 1980, **1**(3), P. 211–221.
- [4] Yamazoe N., Miura N. Environmental gas sensing. *Sensors Actuators*, 1994, **B20**(2), P. 95–102.
- [5] Fergus J.W. The Application of Solid Fluoride Electrolytes in Chemical Sensors. *Sensors Actuators*, 1997, **B42**(2), P. 119–130.
- [6] Miura N., Hisamoto J., Yamazoe N., Kuwata S. LaF_3 sputtered film sensor for detecting oxygen at room temperature. *Applied Surface Science*, 1988, **33/34**, P. 1253–1259.
- [7] Miura N., Hisamoto J., Yamazoe N., Kuwata S., Salardenne J., Solid-state oxygen sensor using sputtered LaF_3 film. *Sensors Actuators*, 1989, **B16**(4), P. 301–310.
- [8] Fedorov P.P., Luginina A.A., Kuznetsov S.V., Osiko V.V. Nanofluorides. *Journal of Fluorine Chemistry*, 2011, **132**(12), P. 1012–1039.
- [9] Trnovcova V., Garashina L.S., Skubla A., Fedorov P.P., Cicka R., Krivandina E.A., Sobolev B.P. Structural aspects of fast ionic conductivity of rare earth fluorides. *Solid State Ionics*, 2003, **157**(1-4), P. 195–201.
- [10] Trnovcova V., Fedorov P.P., Furara I. Fluoride Solid Electrolytes. *Russian Journal of Electrochemistry*, 2009, **45**(6), P. 630–639.

- [11] Guo H., Zhang T., Qiao Y.M., Zhao L.H., Z. Quan Li. Ionic Liquid-Based Approach to Monodisperse Luminescent LaF₃: Ce, Tb Nanodiskettes: Synthesis, Structural and Photoluminescent Properties. *Journal Nanoscience and Nanotech*, 2010, **10**(3), P. 1913–1919.
- [12] Zhang Y., Lu M. Labelling of silica microspheres with fluorescent lanthanide-doped LaF₃ nanocrystals. *Nanotechnology*, 2007, **18**(27), P. 275603.
- [13] Zhu X., Zhang Q., Li Y., Wang H. Redispersible and water-soluble LaF₃: Ce, Tb nanocrystals via a microfluidic reactor with temperature steps. *Journal Material Chemistry*, 2008, **18**(42), P. 5060–5062.
- [14] Mi C.C., Tian Z.H., Han B.F., Mao C., Xu S.K. Microwave-assisted one-pot synthesis of water-soluble rare-earth doped fluoride luminescent nanoparticles with tunable colors. *Journal Alloys Compound*, 2012, **525**, P. 154–158.
- [15] Pieterse L.V., Wegh R.T., Meijerink A. Emission spectra and trends for $4f^{n-1}5d \leftrightarrow 4f^n$ transitions of lanthanide ions: Experiment and theory. *The Journal of Chemical Physics*, 2001, **115**(20), P. 9382.
- [16] Meng J., Zhang M., Liu Y. Hydrothermal preparation and luminescence of LaF₃:Eu³⁺ nanoparticles. *Spectroscopic Acta part A*, 2007, **66**(1), P. 81–85.
- [17] Daihua T., Liu X., Zhen Z. Oleic acid (OA)-modified LaF₃: Er, Yb nanocrystals and their polymer hybrid materials for potential optical-amplification applications. *Journal of Material Chemistry*, 2007, **17**(1), P. 1597–1601.
- [18] Daqin C., Yuansheng W., En Ma, Yunlong Y. Influence of Yb³⁺ content on microstructure and fluorescence of oxyfluoride glass ceramics containing LaF₃ nano-crystals. *Material Chemistry Physics*, 2007, **101**(9), P. 464–469.
- [19] Pi D., Wang F., Fan X., Wang M., Zhang Y. Polyol-mediated synthesis of water-soluble LaF₃:Yb,Er upconversion fluorescent nanocrystals. *Materials Letters*, 2007, **61**(6), P. 1337–1340.
- [20] Yuanfang L., Wei C. Shaopeng W. Alan G.J. Sarah W. Boon K.W. X-ray Luminescence of LaF₃: Tb and LaF₃: Ce, Tb Water Soluble Nanoparticles. *Journal of Applied Physics*, 2008, **103**(6), P. 1–7.
- [21] Wang Z.L., Quan Z.W., Jia P.Y., Lin C.K., Luo Y., Chen Y., Fang J., Zhou W., Connor C.J.O., Lin. A Facile Synthesis and Photoluminescent Properties of Redispersible CeF₃, CeF₃:Tb³⁺, and CeF₃:Tb³⁺ / LaF₃ (Core / Shell) Nanoparticles. *Chemistry of Materials*, 2006, **18**(8), P. 2030–2037.
- [22] Li C., Liu X., Yang P., Zhang C., Lian H., and Lin. LaF₃, CeF₃, CeF₃:Tb³⁺, and CeF₃:Tb³⁺ @ LaF₃ (Core/Shell) Nanoplates: Hydrothermal Synthesis and Luminescence Properties. *The Journal of Physical Chemistry C*, 2008, **112**(8), P. 2904–2910.
- [23] Guo H. Photoluminescent properties of CeF₃:Tb³⁺ nanodiskettes prepared by hydrothermal microemulsion. *Applied Physics B-Lasers Optics*, 2006, **84**(1-2), P. 365–369.
- [24] Kurtz S.K., Perry T.T. A powder technique for the evaluation of nonlinear optical materials. *Journal of Applied Physics*, 1968, **39**(8), P. 3798–3813.